Available online at www.sciencedirect.com
ScienceDirect
Ceramics International 37 (2011) 2803–2808
CERAMICS INTERNATIONAL
www.elsevier.com/locate/ceramint

The synthesis of peculiar structure of spring-like multiwalled carbon nanotubes via mechanothermal method

S.A. Manafi [a,*], M.R. Rahimipour [b], Y. Pajuhanfar [a]

[a] Department of Ceramics, Shahrood Branch, Islamic Azad University, Shahrood, Iran
[b] Materials and Energy Research Center, P.O. Box 14155-4777, Tehran, Iran

Received 16 March 2011; received in revised form 25 April 2011; accepted 25 April 2011
Available online 5 May 2011

Abstract

A simple, economical and convenient mechanothermal process for the synthesis of spring-like multiwalled carbon nanotubes (S-MWCNTs) with advantages of large-quantity production and low cost is described. Interestingly, many peculiar morphologies are reported for the first time as an extraordinary structure from family carbons that could represent unique building blocks for nanoengineering as a result of their special electronic and mechanical properties. As the matter of fact, this special structure guarantees its usage in the world of composites as reinforcement material for good flexible structures. Here, we report the synthesis of S-MWCNTs by annealing amorphous carbon powders at 1380 °C in an Ar atmosphere. The amorphous powders were obtained after ball-milling graphite for times longer than 150 h. The characterization of S-MWCNTs by high resolution transmission electron microscope, scanning electron microscope indicated that S-MWCNTs had uniform tubular hollow structures with openings, a length of about several millimeters, and a diameter of 80 ± 30 nm at the open and closed end. Also, Brunauer–Emmett–Teller indicated surface area as high as ~210 m^2/g. Finally, the magical structure introduced an intermediate structure between two well-known structures as may be of particular interest from both fundamental and applied points of view.

Keywords: Peculiar structure; Carbon nanotubes; Nanotechnology; HRTEM

1. Introduction

Carbon nanotubes have attracted considerable interest since their discovery by Iijima in 1991 [1]. Carbon nanotubes have aroused great interest recently because of their unique physical properties, which span a wide range from structural to electronic. For example, nanotubes have a low weight and high elastic modulus, and thus they are predicted to be the strongest fibers and widely touted as attractive candidates for use as fillers in composite materials due to their extremely high Young's modulus, stiffness, and flexibility [2–6]. These latter applications will require vast quantities of nanotubes at competitive prices to be economically feasible. Moreover, reinforcing applications may not require ultrahigh purity nanotubes. On the other hand, functionalization of nanotubes to facilitate interfacial bonding within composites will naturally introduce defects into the tube walls, lessening morphologies are needed for specified applications of CNTs. For instance, usually it is needed to prepare knotted CNTs to improve in rich interfacial adhesion, which can lead to nanotube aggregation within the matrix composites. So, there are many methods of producing these nanomaterials, including electric arc discharge [1,7], laser evaporation [8], chemical vapor deposition (CVD), catalytic CVD [9–19], hydrothermal treatment [20] and mechanothermal process in which graphite powders were first mechanically ground at room temperature and then annealed at 1400 °C [21], but little is known about the possibilities of mechanothermal processing aimed to the synthesis of carbon nanostructures in different conditions. Although significant research progress has been made to synthesize carbon nanomaterials, but developing an easy approach to large-scale production of carbon nanotubes has still been limited to date. On the other hand, most of the synthesizing methods are complicated and uncontrollable. More recently, we have suggested that using washable supported catalysts is accompanied by valuable advantages and with an extraordinary

* Corresponding author. Tel.: +98 273 333 4530; fax: +98 273 333 4537.
E-mail address: ali_manafi2005@yahoo.com (S.A. Manafi).

0272-8842/$36.00
doi:10.1016/j.ceramint.2011.04.077

structure [22,23]. Herein, we use an efficient method for the controlled synthesis of spring-like multiwall carbon nanotubes by mechanical activation assisted annealed process. Spring-like MWCNTs were fabricated with advantages of mass production, low cost and high-yield without adding any pre-synthesized Fe/Co/Ni nanocatalysts. Finally, we report a simple and convenient synthesis method of CNTs with outstanding morphology structure. This method needs no complicated process, relatively low cost and economically.

2. Experimental procedures

Elemental graphite flakes (99.9% < 100 μm) with a purity of 99.8% were mechanically ground in a purified argon atmosphere. Four grams with ten steel balls of diameter 15 mm were used in the mechanical activation (MA) process. The ball-to-powder weight ratio was kept at 20:1. Mechanical activation was carried out at ambient temperature and at a rotational speed (cup speed) of 700 rpm in a planetary ball mill. The mechanical activation (MA) process was interrupted at regular intervals with a small amount of the MAed powder taken out from the vial to study changes in the microstructures at selected milling duration. The vial containing the powders and the ball were evacuated by a rotary-pump and then back-filled with a pure argon gas (99.99%) in a glove box. The final gas pressure in the vial was kept to be 0.1 MPa. We removed Fe/Cr contamination by treatment with a 30 mL aqueous solution containing 2 mL of hydrochloric acid (36.5 wt.%), 5 mL of H_2O_2 (30 wt.%), and 20 mL of distilled water ($HCl:H_2O_2:H_2O$ = 2:5:20, v/v/v) at room temperature for 12 h.

After full amorphization, the highly chemically active carbon powders were annealed at different temperatures to investigate the formation of multi-walled carbon nanotubes. The crystal phase was determined with powder X-ray diffraction. For these experiments, a Siemens diffractometer (30 kV and 25 mA) with the $K_{\alpha 1}$, radiation of copper (λ = 1.5406 Å), was used. The structural and compositional information of the product materials was obtained with scanning electron microscopy (SEM) and energy-dispersive X-ray spectroscopy (SEM/EDX, XL30), field emission transmission electron microscopy and selected area electron diffraction (FETEM/SAED, Philips CM200 transmission electron microscope operated at 200 kV). Specific surface areas (SSAs) of carbon/carbon nanotubes were also measured by the Brunauer–Emmett–Teller (BET) method. The BET surface areas, S_{BET}, of the samples were determined from N_2 adsorption–desorption isotherms obtained at 77 K using an ASAP 2010 surface area analyzer. The Brunauer–Emmett–Teller (BET) method is the most widely used procedure for the determination of the surface areas of solid materials and involves the use of the BET equation:

$$\frac{1}{W[(P_0/P)-1]} = \frac{1}{W_m C} + \frac{C-1}{W_m C}\left(\frac{P}{P_0}\right) \quad (1)$$

in which W is the weight of gas adsorbed at a relative pressure of P/P_0 and W_m is the weight of adsorbate constituting one monolayer of surface coverage. The term C, the BET C constant, is related to the energy of adsorption in the first adsorbed layer, and consequently, its value is an indication of the magnitude of the adsorbent–adsorbate interactions. When the range of P/P_0 is 0.05–0.35, a line will be obtained. Through the slope and intercept, the adsorbate monolayer saturation amount (V_m) can be obtained. The BET surface area equation is:

$$S_{BET} = \frac{V_m N_0 \sigma}{22,400\ \mathrm{W}} \quad (2)$$

where N_0 is Avogadro's number and σ is the cross-sectional area of a single molecule. Raman spectra were taken at room temperature under ambient condition using an Almega Raman spectrometer with an Ar^+ at an excitation wavelength of 514.5 nm. The crystallite size, D, was estimated by Williamson–Hall [24]:

$$\beta \cos\theta = 2\varepsilon \sin\theta + 0.9\frac{\lambda}{D} \quad (3)$$

where λ is the wavelength of the X-ray, β the full width at half-maximum (FWHM), θ the Bragg angle, and ε is the microstrain.

3. Results and discussion

XRD patterns of graphite powder mechanically mixed in argon atmosphere for several activation times are shown in Fig. 1. Further milling (after 150 h MA) caused no change in XRD patterns except the broadening of the peaks. So, this broadening can be attributed to the decrease of grain size and increasing of strain in the lattice. A peak at about 15° in the XRD pattern can be seen that it possesses to sample holder. In general we can conclude that this method is very successful method for amorphous of graphite powders by mechanical activation (MA).

The constitution of this starting powder corresponds to the elemental graphite powder. The diffraction intensities drastically decreased after mechanical activation (MA). The diffraction peaks corresponding to the graphite (particularly the peak at about 2θ = 29°) almost disappeared at an activating time of 10 h. The crystallite size of the graphite after mechanical activation for 5 h are approximately D = 30.1 nm where that before MA it is approximately D = 31.1 (Table 1).

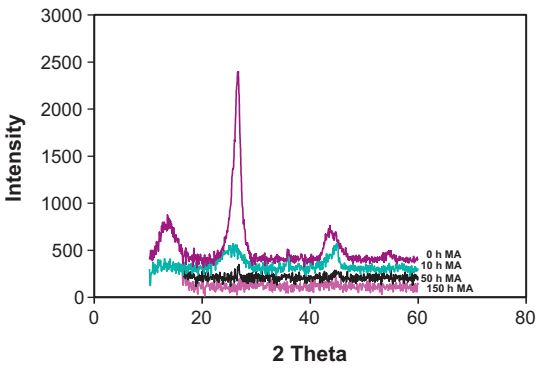

Fig. 1. The X-ray diffraction spectra of mechanically alloyed graphite powders at different milling times.

Table 1
Characteristic of different samples used to investigate during milling.

Milling time (h)	Sample (Id)	S.A. (m^2/g)	Crystallite size, D (nm)
0	C_0	5.5	31.1
5	C_5	21.2	30.1
10	C_{10}	25.8	29.8
30	C_{30}	35.1	27.4
50	C_{50}	45.6	25.4
60	C_{60}	50.1	24.6
80	C_{80}	62.5	22.1
90	C_{90}	70.2	20.1
100	C_{100}	78.9	18.5
120	C_{120}	115.2	13.9
130	C_{130}	145.2	11.2
140	C_{140}	175.5	8.5
150	C_{150}	200.5	5.2
160	C_{160}	205.5	4.9
170	C_{170}	207.4	4.8
180	C_{180}	209.1	4.7
190	C_{190}	209.5	4.8
200	C_{200}	211.2	4.8
210	C_{210}	211.2	4.8
220	C_{220}	211.2	4.8

D is the average crystallite size, determined by the Williamson–Hall; S.A. is the specific surface area, determined by the BET-method.

An additional MA process in the argon atmosphere (Fig. 1), diffraction intensities corresponding to the graphite decrease gradually with increasing activating time, at the diffraction peaks at around $2\theta = 29^\circ$ cannot be eliminated after an activating time of 100 h, suggesting that the formation of an amorphous-like phase or very fine particles has been strongly enhanced in the argon atmosphere after an activating time of 150 h. Fig. 2 shows the transmission electron micrograph and selected area electron diffraction pattern of graphite nanostructures synthesizing according to the method described above. It is readily observed that the nanostructures are in a high ultra-fine dispersion and the average crystalline size is 10 nm.

The electron diffraction (ED) pattern of the carbon nanotubes (Fig. 2) exhibits two very weak diffuse rings, indicating highly disordered wall milled graphite. On the other hand, the electron diffraction pattern reveals that the carbon nanostructures have an amorphous structure. At the same time, this result is consistent with the X-ray diffraction (XRD) pattern. We believe that the very small size and the amorphous structure are due to the high energy ball milling of the graphite powders activated by planetary mill. Also, Jiang and Chen recently developed a thermodynamic quantitative model to describe the phase transitions of nanocarbon as functions of its size and temperature through systematically considering the effects of surface stresses and surface energies. The fine nanosize amorphous structure of pure carbon nanostructures is thermodynamically unstable, owing to the high amount of free energy. Therefore, crystallization at a temperature regime might be expected.

The milled powders had an average crystallite size of about 5–10 nm as determined by the Williamson–Hall method as shown in Table 1. Crystallite size values determined in this way may be low when the concentration of defects in the sample in higher compared to that in the reference large-particulate powder. The BET areas are strongly different for all samples, and between 5.5 and 211.2 m^2/g as presented in Table 1. In the steady state, the BET surface area of the MAed powders was determined at about 211.2 m^2/g for several samples (C_{200}, C_{210}, C_{220} and ...).

Measuring the surface area of carbon nanostructures via nitrogen adsorption by Brunauer–Emmet–Teller (BET) method revealed a specific surface area of 211.2 m^2/g which seems relevant for surface area dependent applications such as diffusion process. Assuming that all particles are spherical and theoretical density, and form: $d_{BET} = 6/S{\cdot}\rho$, where S is the surface area and ρ is the particle density (2.1 g/cm^3 for graphite), a BET particle diameter, d_{BET}, of about 20 nm is found for these nanoparticles. At the same time, there results are consistent with the HRTEM image observations. So, these (S.A., and D) indicate at particulate are highly chemically active carbon atoms.

According to HRTEM micrographs of the powders mechanically milled for 150 h in argon gas atmosphere are shown in Fig. 3, that MAed powders are an ultra-fine spherical particle powder with approximately 100 ± 20 nm in size. Because, highly chemically active carbon atoms, these are strongly agglomerated.

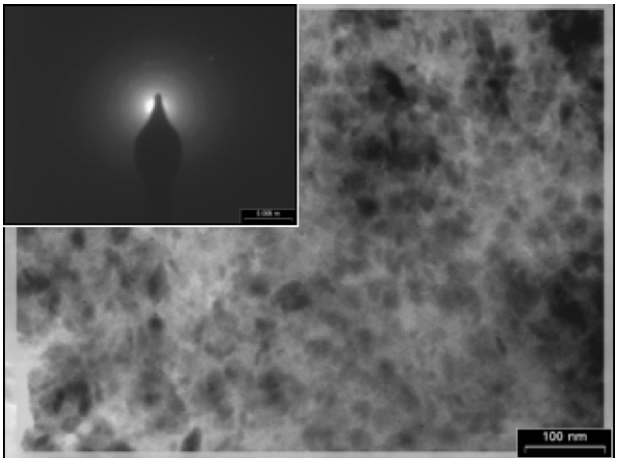

Fig. 2. Transmission electron microscope of materials obtained by a mechanical activation with selected area electron diffraction pattern.

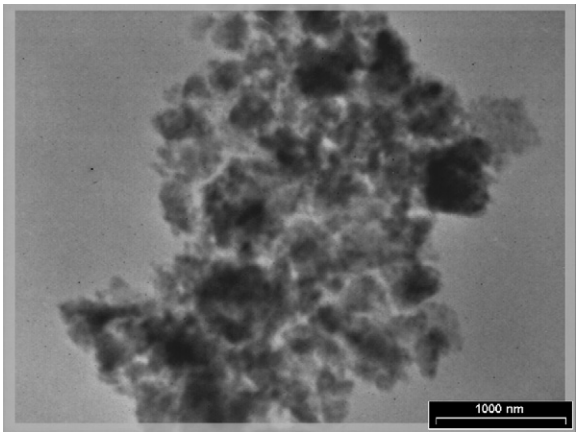

Fig. 3. MAed graphite powders for 150 h in argon gas atmosphere.

Interestingly, Fig. 4(a–e) shows the SEM different images of MAed graphite powders (the sample of C_{150}) after annealing at different temperatures. SEM observations in a wide field show that the powders prepared with the heat-treated (C_{150}) contain much more nanotubes with peculiar structure viz. spring-like multiwall carbon nanotubes (S-MWCNTs). The nanotubes are knotted and stretchy in appearance, and are mainly S-MWCNTs which will be demonstrated later. In the SEM observation of C_{150}, a few carbon nanotubes (CNTs) were sporadically observed. However, for the sample C_{70}, C_{90}, and C_{100}, no CNTs or MWCNTs were found in all observations after annealing at 1380 °C. The spring-like morphology of the multiwall carbon nanotubes was well maintained after the high-temperature treatment. A detailed study of the growth mechanism of the S-MWCNTs is underway. The interesting structure and physical properties (high aspect ratio ca. 1000 and low density) of the S-MWCNTs make it an obvious choice as fillers/reinforcing components in composites.

Finally, in this investigation, an effective method was developed for the formation of ultra-crystallinity spring-like MWCNTs. The S-MWCNTs are high aspect-ratio, high-crystalline and uniformly structured. As the matter of fact, this method (mechanothermal method) guarantees its production in the synthesis of CNT for different applications. Fig. 4(e) shows a high magnification SEM image of a typical S-MWCNT with an ultra-high crystallinity structure.

Meanwhile, TEM images of mechanically activated graphite powders after annealing at 1380 °C show in Fig. 5(a and b). In Fig. 5(a), many S-MWCNTs can be observed, which is consistent with the SEM observation. By TEM observation, we have found that most of nanotubes in the annealed powders are S-MWCNTs. Fig. 5(b) shows TEM image of individual hollow MWCNTs (C_{150}). The average diameter of resultant the spring-like MWCNTs was a length of about several millimeters, and a diameter of 80 ± 30 nm at the open and closed end. Also, we confirmed that the carbon nanotube is spring-like shaped. Spring-like shaped MWCNTs

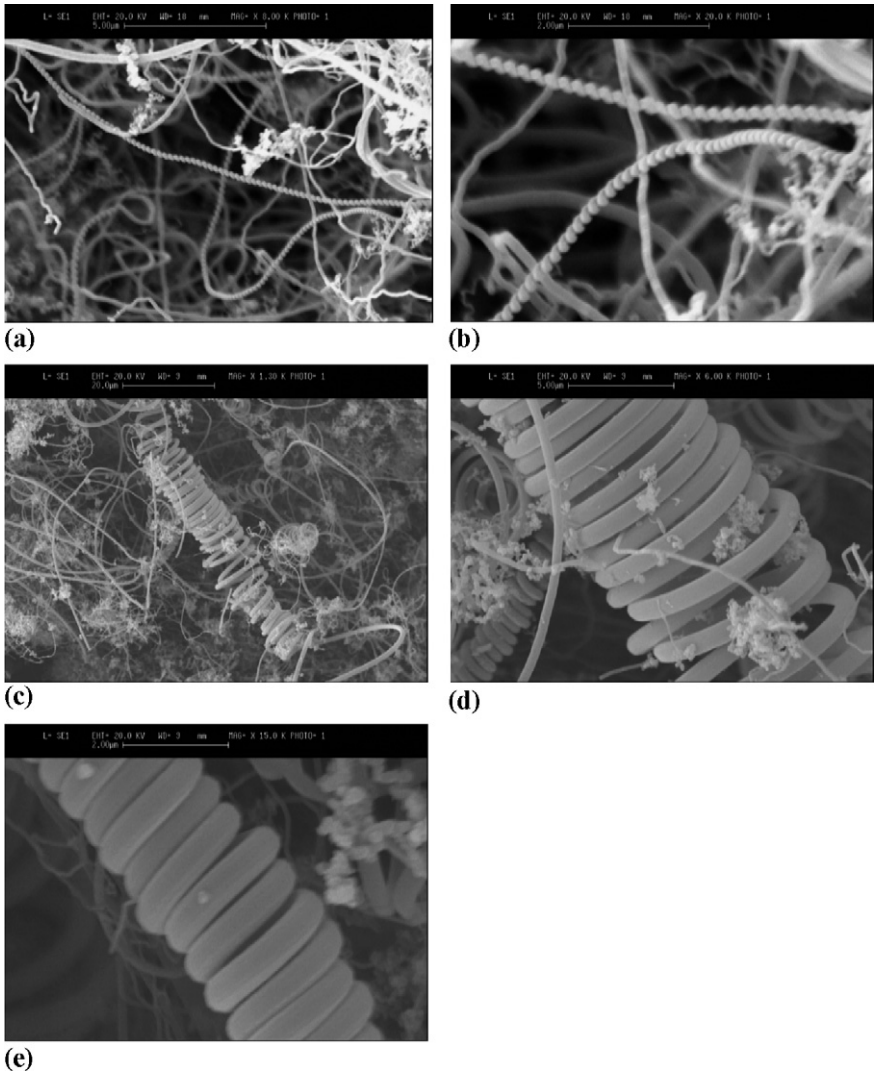

Fig. 4. SEM images of MAed graphite powders for 150 h after annealing at 1380 °C with different morphologies, (a) high yield spring-like MWCNTs, (b) spring-like MWCNTs with high magnification, (c) spring-like MWCNTs encapsulated with carbon nanotubes, (d) spring-like MWCNTs encapsulated with bundle carbon particles, and (e) S-MWCNT with an ultra-high crystallinity structure.

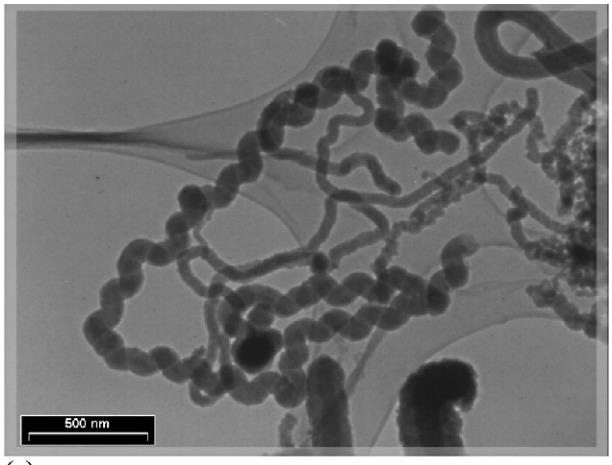

(a)

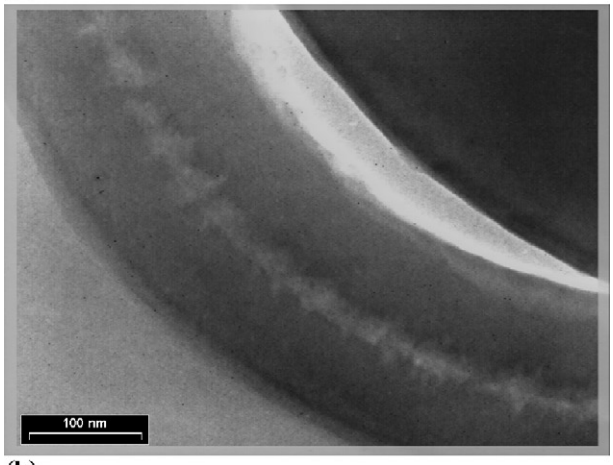

(b)

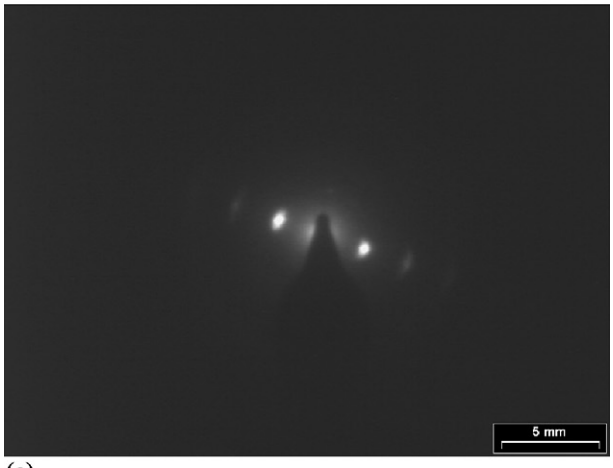

(c)

Fig. 5. HRTEM images of MAed graphite powders for 150 h after annealing at 1380 °C, (a) low magnification, (b) hollow MWCNT with high magnification, and (c) the selected area electron diffraction pattern of the obtained MWCNTs.

with a peculiar structure can also be observed from the inset of Fig. 5(b). The selected area electron diffraction (SAED) pattern (Fig. 5(c)) exhibits a pair of small but strong spots for (0 0 2), together with a ring for (1 0 0) and a pair of weak arcs for (0 0 4) diffractions. The appearance of (0 0 2) diffractions as a pair of spots indicates some orientation of the (0 0 2) planes in the carbon nanotubes [25].

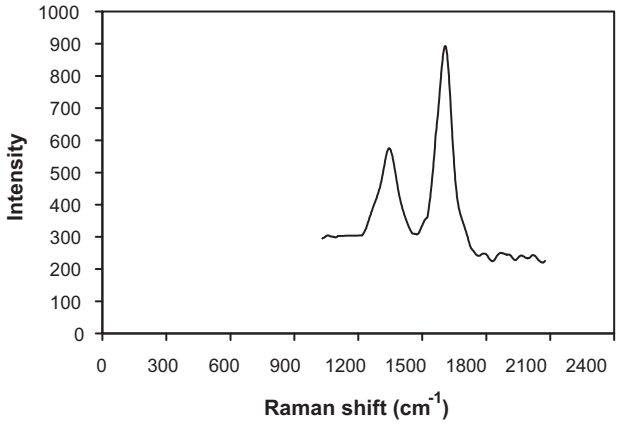

Fig. 6. Raman spectra of the obtained MWCNTs.

The Raman spectrum is shown in Fig. 6, displaying the characteristic wide D and G bands at around 1360 and 1590 cm^{-1}, respectively, typical of amorphous carbons or disordered graphite [26,27]. The peak at 1581 cm^{-1} (G-band) corresponds to a E_{2g} mode of graphite and is related to the vibration of sp^2-bonded carbon atoms in a two-dimensional hexagonal lattice, such as in a graphite layer [27–29]. Nanotubes with concentric multiwalled layers of hexagonal carbon lattice display the same vibration [30]. The D-band at around 1360 cm^{-1} is associated with vibrations of carbon atoms with dangling bonds in plane terminations of disordered graphite or glassy carbons. After treatment, the D-band nearly disappeared and the G-band sharpened, so the relative intensity of the G-band with respect to the D-band increased very significantly. The inverse of the I_D/I_G intensity ratio between G and D bands is an usual measurement of the graphitic ordering and may also indicate the approximate layer size in the hexagonal plane, La [27,31], which in this case is related to the length of pristine (defect-free) graphitic multiwalls. The I_D/I_G ratio in the treated material is ~0.03, compared to a value of ~0.9 in the starting material. The calculation using the relationship La) 44 $(I_D/I_G)^{-1}$ yields values of around 1.5 μm for the treated sample, in good agreement with the maximum length of multiwall carbon nanotubes observed in TEM images. The sharp decrease of I_D/I_G indicates that the number of sp^2 bonded carbon atoms without dangling bonds have increased at the expense of disordered carbon. The low ratio I_D/I_G is characteristic of a graphite lattice with perfect two-dimensional order in the basal plane. The spectrum in Fig. 6 indicates a nearly defect-free lattice ordering, and reveals that the multiwalls forming the nanotubes have a perfect lattice without defects, edges, or plane terminations. The crystallinity of mechanothermal (MT) nanotubes is similar or higher than in multiwall nanotubes grown using evaporation methods, for which I_D/I_G ratios are typically ~0.10.

4. Conclusion

In the content of this preliminary paper, we have successfully synthesized spring-like MWCNTs via a mechanothermal (MT) process at 1380 °C, without any speculation

about the mechanism. We believe this work will significantly advance the incorporation of nanomaterials for future studies. This is also accompanied by the appearance of an interesting phenomenon, viz. formation of spring-like of peculiar carbon nanotubes. The report result are of general interest, and may be the beginning point of various researches such as investigation of composite of this unique reinforcement materials, inspecting the mechanism of formation, application of this outstanding nanostructure for nanotechnological purpose, etc. The purity and good quality of S-MWCNTs obtained by mechanothermal make suitable synthesis a promising method for the production of multiwall carbon nanotubes or other graphitic nanocarbons.

Acknowledgements

The authors thank the Tarbit Modarres University for access to Raman spectroscopy and technical support. So, the authors would like to acknowledge Dr. Hesari for investigating TEM image, Professor Torabi for helping in preparing of this paper and Mr. Jabbari for performing the experimental tests.

References

[1] S. Iijima, Helical microtubules of graphitic carbon, Nature 6348 (1991) 56.
[2] M. Ouyang, J.L. Huang, C.M. Lieber, Fundamental electronic properties and applications of single-walled carbon nanotubes, Acc. Chem. Res. 12 (2002) 1018.
[3] M.M.J. Treacy, T.W. Ebbesen, J.M. Gibson, Exceptionally high Young's modulus observed for individual carbon nanotubes, Nature 6584 (1996) 678.
[4] Y.F. Yin, T. Mays, B. McEnaney, Adsorption of nitrogen in carbon nanotube arrays, Langmuir 25 (1999) 8714.
[5] D. Li, Y. Xia, Direct fabrication of composite and ceramic hollow nanofibers by electrospinning, Nano Lett. 5 (2004) 933.
[6] Y.H. Li, J. Ding, Z. Luan, Z. Di, Y. Zhu, C. Xu, Competitive adsorption of Pb^{2+}, Cu^{2+} and Cd^{2+} ions from aqueous solutions by multiwalled carbon nanotubes, Carbon 14 (2003) 2787.
[7] D. Bethune, C. Kiang, M. deVries, G. Gorman, R. Savoy, J. Vazquez, Cobalt-catalysed growth of carbon nanotubes with single atomic layer walls, Nature 363 (1993) 605.
[8] T. Guo, P. Nikolaev, A. Thess, D. Colbert, R. Smalley, Catalytic growth of single-walled nanotubes by laser vaporization, Chem. Phys. Lett. 243 (1995) 49.
[9] Y.M. Shyu, F.C.N. Hong, The effects of pre-treatment and catalyst composition on growth of carbon nanofibers at low temperature, Diam. Relat. Mater. 7 (2001) 1241.
[10] J.M. Ting, N.Z. Huang, Thickening of chemical vapor deposited carbon fiber, Carbon 6 (2001) 835.
[11] M. Ritschel, M. Uhlemann, O. Gutfleisch, A. Leonhardt, C.A. Graff, J. Fink, Hydrogen storage in different carbon nanostructures, Appl. Phys. Lett. 16 (2002) 2985.
[12] V. Ivanov, J.B. Nagy, P. Lambin, A. Lucas, X.B. Zhang, X.F. Zhang, The study of carbon nanotubes produced by catalytic method, Chem. Phys. Lett. 4 (1994) 329.
[13] V. Vinciguerra, F. Buonocore, G. Panzera, L. Occhipinti, Growth mechanisms in chemical vapour deposited carbon nanotubes, Nanotechnology 6 (2003) 655.
[14] E. Couteau, K. Hernadi, J.W. Seo, C. Bonjour, L. Forro, R. Schaller, CVD synthesis of high-purity multiwalled carbon nanotubes using $CaCO_3$ catalyst support for large-scale production, Chem. Phys. Lett. 2 (2003) 9.
[15] D. Lupu, A.R. Biris, A. Jianu, C. Bunescu, E. Burkel, E. Indrea, Carbon nanostructures produced by CCVD with induction heating, Carbon 3 (2004) 503.
[16] A. Okamoto, H. Shinohara, Control of diameter distribution of single-walled carbon nanotubes using the zeolite CCVD method at atmospheric pressure, Carbon 2 (2005) 431.
[17] L. Piao, Y. Li, J. Chen, L. Chang, J.Y. Lin, Methane decomposition to carbon nanotubes and hydrogen on an alumina supported nickel aerogel catalyst, Catal. Today 2 (2002) 145.
[18] M. Yudasaka, R. Kikuchi, T. Matsui, Y. Ohki, S. Yoshimura, E. Ota, Specific conditions for Ni catalyzed carbon nanotube growth by chemical vapor deposition, Appl. Phys. Lett. 67 (1995) 2477.
[19] M. Shaijumon, S. Ramaprabhu, Synthesis of carbon nanotubes by pyrolysis of acetylene using alloy hydride materials as catalysts and their hydrogen adsorption studies, Chem. Phys. Lett. 374 (2003) 513.
[20] J. Maria, C. Moreno, M. Yoshimura, Hydrothermal processing of high-quality multiwall nanotubes from amorphous carbon, J. Am. Chem. Soc. 123 (2001) 741.
[21] Y. Chen, M.J. Conway, J.D. Fitzgerald, Carbon nanotubes formed in graphite after mechanical grinding and thermal annealing, Appl. Phys. A 76 (2003) 633.
[22] S.A. Manafi, S.H. Badiee, Production of carbon nanofibers using a CVD method with lithium fluoride as a supported cobalt catalyst, Res. Lett. Mater. Sci. 1 (2008) 1.
[23] A. Eftekhari, S.A. Manafi, F. Moztarzadeh, Catalytic chemical vapor deposition preparation of multi-wall carbon nanotubes with cone-like heads, Chem. Lett. 35 (2006) 138.
[24] G.K. Williamson, W.H. Hall, X-ray line broadening from filled Al and W, Acta Metall. Sin. 1 (1953) 22.
[25] W. Wang, S. Kunwar, J.Y. Huang, D.Z. Wang, Z.F. Ren, Low temperature solvothermal synthesis of multiwall carbon nanotubes, Nanotechnology 16 (2005) 21.
[26] C.A. Dyke, J.M. Tour, Overcoming the insolubility of carbon nanotubes through high degrees of sidewall functionalization, Chem. Eur. J. 10 (2004) 812.
[27] R. Saito, A. Jorio, G. Antonio, G. Dresselhaus, S. Mildred, A.G. Dresselhaus, First and second-order resonance Raman process in graphite and single wall carbon nanotubes, Jpn. J. Appl. Phys. 41 (2002) 4878.
[28] S.A. Maher, Raman spectroscopy and molecular simulation investigations of adsorption on the surface of single-walled carbon nanotubes and nanospheres, J. Raman Spectrosc. 6 (2007) 721.
[29] T. Maruyama, T. Shiraiwa, N. Fujita, Y. Kawamura, S. Naritsuka, M. Kusunoki, Characterization of small-diameter carbon nanotubes and carbon nanocaps on SiC(0001) using Raman spectroscopy, Jpn. J. Appl. Phys. Part 1 45 (2006) 7231.
[30] L.G. Cancado, K. Takai, T. Enoki, M. Endo, Y.A. Kim, H. Mizusaki, Measuring the degree of stacking order in graphite by Raman spectroscopy, Carbon 2 (2008) 272.
[31] L.G. Cancado, K. Takai, T. Enoki, M. Endo, Y.A. Kim, H. Mizusaki, Measuring the degree of stacking order in graphite by Raman spectroscopy, Carbon 46 (2008) 272.